

# Microscopic dynamics of the glass transition investigated by time-resolved fluorescence measurements of doped chromophores

Jing Yong Ye,\* Toshiaki Hattori, and Hiroki Nakatsuka

*Institute of Applied Physics, University of Tsukuba, Tsukuba, Ibaraki 305, Japan*

Yoshihiro Maruyama and Mitsuru Ishikawa\*

*Hamamatsu Photonics Tsukuba Research Laboratory, Tsukuba, Ibaraki 300-26, Japan*

(Received 11 April 1997)

The microscopic dynamics of several monomeric and polymeric glass-forming materials has been investigated by time-resolved fluorescence measurements of doped malachite green molecules in a wide temperature region. For monomers, 1-propanol, propylene glycol, and glycerol, and a polymer without side chains, polybutadiene, the temperature dependence of nonradiative decay time of doped malachite green molecules behaves in a similar way through the glass-transition region. Besides a kink around the calorimetric glass-transition temperature  $T_g$ , another crossover at a critical temperature  $T_c$  about 30–50 K above  $T_g$  has been clearly observed. This experimental finding is in agreement with the prediction of the mode-coupling theory that a dynamical transition exists well above  $T_g$ . On the other hand, for the complex polymers with side chains, poly(vinyl acetate), poly(methyl acrylate), and poly(ethyl methacrylate), the crossover at  $T_g$  is less pronounced than those for the monomers and the polymer without side chains. Moreover, although we could not distinguish any singularities above  $T_g$  for these complex polymers, we observed another kink below  $T_g$ , which may be attributed to the side-chain motions. [S0163-1829(97)02333-3]

## I. INTRODUCTION

The process of glass formation has attracted much attention and has been extensively studied for many years, since it is of both academic and practical importance. However, it is still one of the major poorly understood subjects in condensed-matter physics because of its complex nature. A fundamental problem, that no significant difference in the structure is found between the glassy and liquid states, remained a mystery for long time until an explanation was given by mode-coupling theory (MCT),<sup>1-3</sup> in which a dynamical glass transition from ergodicity to nonergodicity is predicted to occur. Starting from a generalized oscillator equation of motion for the density autocorrelation function containing a nonlinear memory term, without assuming any singularities for the static structure factor, MCT shows that molecules in a supercooled liquid become trapped by their neighbors in cages and the cages ultimately become frozen at a critical temperature  $T_c$  well above the calorimetric glass-transition temperature  $T_g$ . Above  $T_c$  the density correlation function is said to perform a two-step decay; i.e., a fast local relaxation,  $\beta$  process, is followed by a slow primary-structural relaxation,  $\alpha$  process. According to the idealized version of MCT, the  $\alpha$  process is slowed down dramatically with decreasing temperature until it does not occur any more at and below  $T_c$ , so that the density correlation function does not decay to zero even if we wait for an infinitely long time, although the  $\beta$  process still remains. Thus the theory describes a dynamical transition from an ergodic liquid to a nonergodic glass at  $T_c$ .

The theoretical progress stimulated intensive studies of the glass transition in a dynamical window, i.e., in a mesoscopic time regime and on a microscopic length scale,

which is significantly different from the conventional macroscopic studies like viscosity measurement and calorimetric measurement, etc. Especially, typical fragile glass-forming monomers have been studied by many researchers by means of neutron-<sup>4-9</sup> and light-scattering<sup>10-14</sup> measurements, and the experimental results are in a good agreement with the predictions of MCT. However, studies on the glass transition of associated glass-forming monomers such as alcoholic glasses, which can, in general, form glass very easily and are much more important in application, do not seem to be so successful thus far. Only a few studies on the associated glass formers were reported,<sup>15-17</sup> and the critical temperature  $T_c$  obtained for a same sample scatters in a wide temperature range. The deviation from the prediction of MCT was attributed to the contribution of intramolecular and intermolecular vibrational modes. Our previous study<sup>18</sup> suggested that in monomeric associated solvents the crossover phenomena at  $T_c$  can be clearly observed by a microscopic probe which is sensitive to the density fluctuation on a microscopic scale and less coupled to the thermally activated hopping process, which is important in the determination of the properties of solvents on a comparably large scale. In cases of polymeric glass formers, polybutadiene, a polymer without side chains, is one of the most extensively studied samples due to its simple molecular structure, and the experimental results have been well analyzed on the basis of MCT.<sup>19-21</sup> However, for the complex polymers containing side chains, the applicability of MCT is still a question open to debate.<sup>22-25</sup> In the present study, we have investigated the dynamics of various kinds of glass-forming systems including associated monomeric solvents and polymers with and without side chains. Comparisons are made between different materials, and the microscopic dynamics has been found to be dependent on the molecular structure of materials.

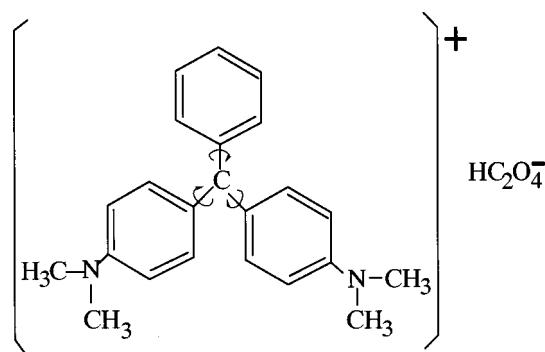


FIG. 1. Molecular structure of malachite green

Time-resolved fluorescence measurements of doped chromophores have been performed to investigate the dynamics of glass transition in the present study. It is known that some chromophores can serve as good local probes to investigate molecular motions and microstructures of liquid and solid matrices.<sup>26–31</sup> The fluorescent probe technique is sensitive in the study of microscopic dynamics since even very weak fluorescence can be well detected with the present technology. Furthermore, with the development of the ultrafast laser technique in recent years, transient fluorescence is possible to be detected even in the femtosecond time regime. Therefore, the dynamics of the glass transition is expected to be investigated by means of fluorescence measurements in a wide time window. In addition, the fluorescence measurement is relatively simple, and its signal-to-noise ratio is generally higher than that of a neutron-scattering measurement.

In this study, malachite green (MG), a kind of triphenylmethane dye, has been used as a molecular probe to monitor the dynamics of the glass transition. The molecular structure of MG is shown in Fig. 1, where three phenyl rings are joined by the central carbon atom. It is known that the rotational motion of the three phenyl rings around the central carbon bonds is the rate-limiting process of the decay of the excited state  $S_1$ , and the fluorescence lifetime varies by several orders of magnitude with the viscosity of the solvent or host matrix.<sup>18,32–34</sup> The internal potential for the rotational motion of the phenyl rings has been shown to be barrierless and flat when a MG molecule is in the  $S_1$  excited state.<sup>32–34</sup> This special nature makes MG a very sensitive molecular probe, since the friction given by the surrounding molecules is the only impediment to the rotational motion of the phenyl rings. Furthermore, the required rotational angle of the phenyl rings for the internal conversion from the  $S_1$  excited state to the ground state is very small (about  $10^\circ$ ), which assures MG to serve as a sensitive probe on a microscopic length scale, i.e., on the order of several angstroms. Owing to the above facts, i.e., the barrierless internal potential and small-scale rotational motions of phenyl rings, the nonradiative decay of MG even in supercooled liquids is so fast that it just falls in the mesoscopic time range, i.e.,  $10^{-11}$ – $10^{-8}$  s, which is predicted by MCT as the relevant dynamical window for the observation of transition from the viscous liquid to the glassy solid. Therefore, one can expect that MG can be used as a unique probe to investigate the microscopic dynamics of the glass transition.

## II. EXPERIMENT

The three selected glass-forming monomers, 1-propanol (PR), propylene glycol (PG), and glycerol (GL), are associated solvents. The calorimetric glass transition temperatures of PR, PG, and GL are reported to be 100, 172, and 193 K, respectively.<sup>35</sup> The preparation of the monomeric samples was described in our previous paper.<sup>18</sup> On the other hand, *cis-trans-vinyl* (36:55:9) polybutadiene (PB) (by Aldrich), with a molecular weight  $M_w = 4.2 \times 10^5$  and the calorimetric glass transition temperature  $T_g = 178$  K, is one of the polymeric glass-forming solvents used in this study. This polymer consists only of a backbone without side chains. The other three polymers, poly(vinyl acetate) (PVAc), poly(methyl acrylate) (PMA), and poly(ethyl methacrylate) (PEMA) (all by Aldrich), contain side chains in contrast to PB. The calorimetric glass-transition temperatures are 303, 282, and 336 K, and the molecular weights  $M_w$  are  $1.67 \times 10^5$ ,  $4 \times 10^4$ , and  $5.15 \times 10^5$  for PVAc, PMA, and PEMA, respectively. The preparation of polymer film samples was as follows: First, 1 mg MG was mixed with 40 ml methylene chloride, and the solution was further mixed with 10 g polymer. After being well mixed, the solution was poured on a glass plate and left to dry naturally for about 4 weeks and kept in a vacuum environment for several hours for further drying. Then a film sample with about 0.2 mm in thickness was obtained.

Each sample, mounted in a cryostat, was first cooled down from room temperature to 10 K at a rate of 2 K/min, and then the fluorescence lifetime was measured from the lowest to the highest temperature step by step. The cw mode-locked pulses from a Nd:YAG laser (Coherent, Antares) were frequency doubled and then used to synchronously pump a mode-locked dye laser (Coherent, Satori) at a repetition rate of 76 MHz. The output pulses from the dye laser with 250-fs pulse width at 642-nm wavelength were attenuated to a few milliwatts and focused on the sample mounted in the cryostat. The emitted fluorescence was wavelength resolved by a spectrometer and time resolved by a synchroscan streak camera (Hamamatsu Photonics, model M1955). The time resolution of the whole apparatus is about 25 ps. No wavelength dependence of the fluorescence decay was found in our experiment, and then the observing wavelength window was selected to be from 674 to 692 nm. As an example, the fluorescence decay curves of MG in PB taken with this system are shown in Fig. 2(a). In the measurement of the slow decay at low temperatures, a different experimental system was employed. A cw mode-locked argon ion laser (Spectra-Physics, model 2030) served as a pump source for a sync-pumped dye laser (Spectra-Physics, model 375B) cavity dumped at a repetition rate of 4 MHz. The output pulses with about 20-ps pulse width were attenuated to a few milliwatts and focused on the sample kept in the cryostat. The emitted fluorescence was detected with a spectrometer (Chromex, 250IS) attached to a photon-counting streak scope (Hamamatsu, C4334). The fluorescence decay curves of MG in PB taken with this system are shown in Fig. 2(b).

## III. EXPERIMENTAL RESULTS

### A. Monomeric samples

For each of the three monomeric samples, the fluorescence decay curves of MG in the low-temperature range are

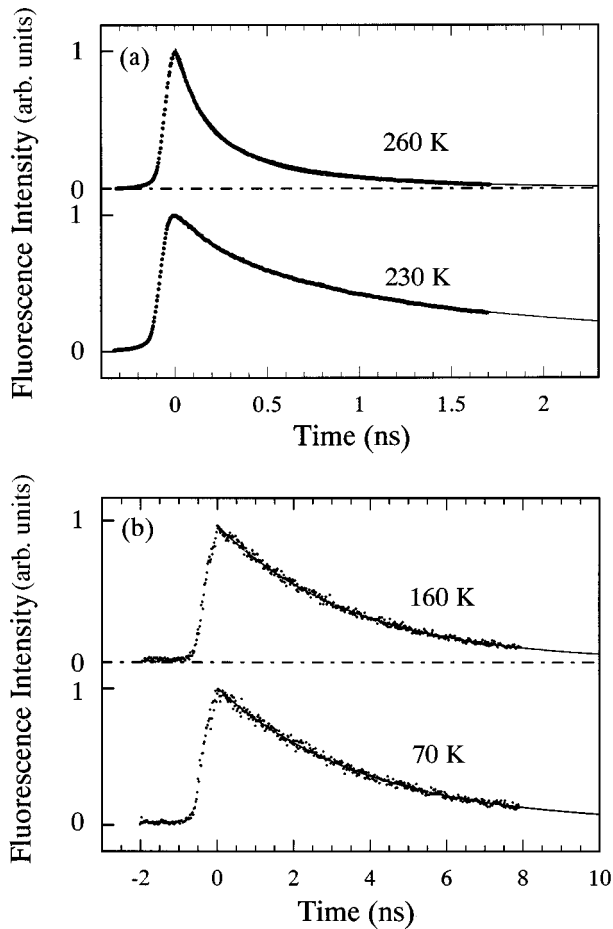


FIG. 2. Fluorescence decay curves of MG doped in PB measured by using the two experimental systems described in the text. Dots are the experimentally obtained data, and solid lines are fitting curves. (a) In the higher-temperature region biexponential decay is found. (b) In the lower-temperature region the decay curves are well fitted to single-exponential functions.

well expressed by single-exponential functions. When the temperature is somewhat above the calorimetric glass-transition temperature  $T_g$ , the decay curve cannot be fitted to a single exponential any more due to the onset of a fast decay component and cannot be fitted to a single-stretched-exponential function either, but can be well fitted to a biexponential function  $I(t) = A_f \exp(-t/\tau_f) + A_s \exp(-t/\tau_s)$ , with two time constants  $\tau_f$  and  $\tau_s$ , and amplitudes  $A_f$  and  $A_s$ . Figure 3 shows the temperature dependence of the fluorescence lifetime of the slow and fast decay components of MG in PR, PG, and GL. The arrows indicate the calorimetric glass-transition temperature  $T_g$ 's for the three samples. The fluorescence lifetime becomes shorter with increasing temperature, and a fast decay component appears from a temperature somewhat above  $T_g$ . For the slow decay component, one can notice that a kink appears at  $T_g$ , and besides that, a singularity point exists at a temperature several tens degrees higher than  $T_g$  for each sample. On the other hand, the amplitude ratios between the fast and slow decay components are shown in Fig. 4 as functions of temperature. The temperature dependences of the amplitude ratios for the three samples are very similar. For each sample the ratio reduces

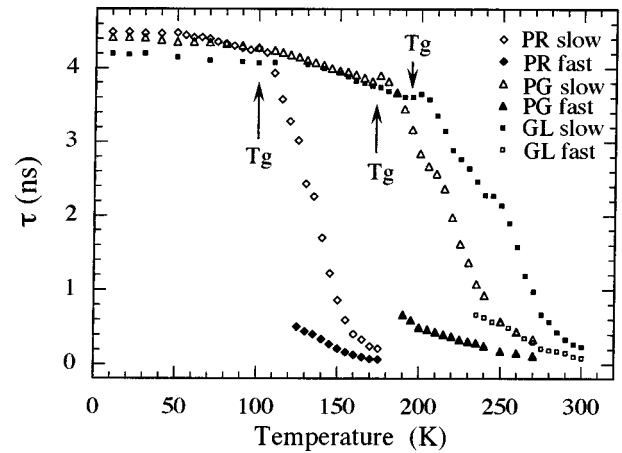


FIG. 3. Temperature dependence of the fluorescence lifetime of MG in PR, PG, and GL.

with decreasing temperature, and the fast decay component practically disappears when the temperature approaches  $T_g$ .

### B. Polymeric samples

For PB, a polymer without side chains, the fluorescence decay curves of doped MG in the high-temperature region are neither single-exponential functions nor single-stretched-exponential functions, but can be well fitted to biexponential functions. The amplitude of the fast decay component reduces with decreasing temperature. When the temperature is lower than  $T_g + 20$  K, the fast decay component decreases to be less than 5% in amplitude and cannot be well resolved from the fluorescence decay curves; then, the decay curves at low temperatures are well fitted to single-exponential functions. The fluorescence lifetime of MG doped in PB is shown in Fig. 5 as a function of temperature. The solid circles represent the fluorescence lifetime of the slow decay component, while the open circles denote the fluorescence lifetime of the fast decay component, which appears from a temperature somewhat above  $T_g$ . For the slow decay component, besides a kink at  $T_g$ , another singularity point can be seen at

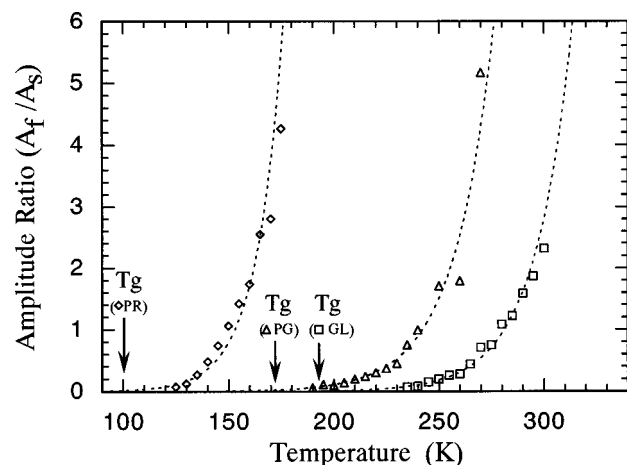


FIG. 4. Amplitude ratios between the fast and slow decay components of MG in PR, PG, and GL are shown as functions of temperature.

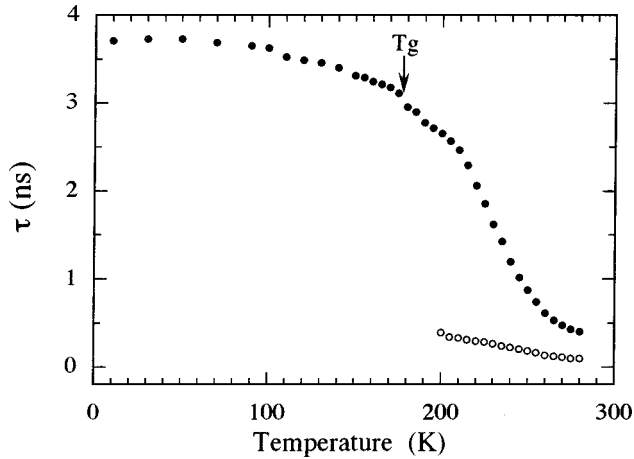


FIG. 5. Temperature dependence of the fluorescence lifetime of MG in PB.

a temperature about 30 K higher than  $T_g$ . On the other hand, Fig. 6 shows the amplitude ratio between the fast and slow decay components as a function of temperature, where the fast decay component gradually disappears when the temperature approaches  $T_g$ . One can notice that all these results of PB are very similar to those of the monomeric samples PR, PG, and GL.

In the cases of PVAc, PMA, and PEMA, all the three polymers contain side chains unlike PB. The fluorescence lifetime of MG doped in these polymers is shown as functions of temperature in Fig. 7. In sharp contrast to the monomers and PB, for each of these samples the fluorescence lifetime of the slow decay component significantly changes even below  $T_g$ , while the kink around  $T_g$  is not so pronounced as those for the monomeric samples and PB. Moreover, we could not clearly distinguish any singularities above  $T_g$ . Figure 8 shows the amplitude ratios between the fast and slow decay components as functions of temperature, where the fast decay component still remains at  $T_g$  and slowly reduces with decreasing temperature until very low temperatures. This temperature dependence of the amplitude ratios is also very much different from that for the monomeric samples and PB, a polymer without side chains.

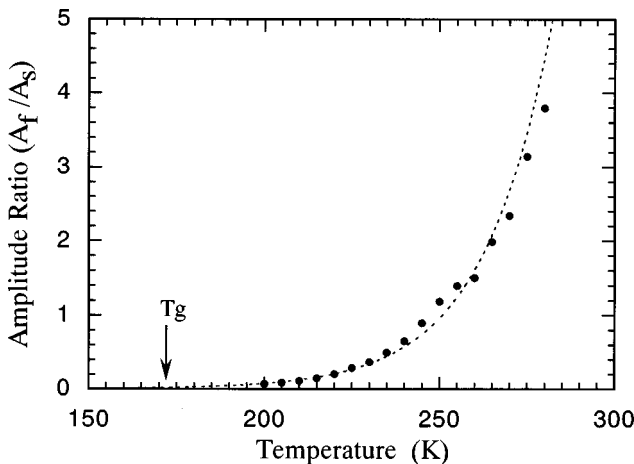


FIG. 6. Amplitude ratio between the fast and slow decay components of MG in PB is shown as a function of temperature.

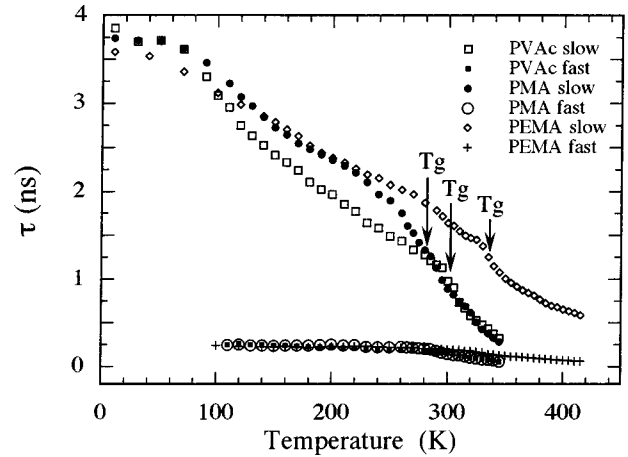


FIG. 7. Temperature dependence of the fluorescence lifetime of MG in PVAc, PMA, and PEMA.

#### IV. DISCUSSION

The process of the fluorescence decay involves the radiative and nonradiative decay channels, in which the radiative decay is reasonably assumed to be unrelated with relaxation processes of the host matrix and independent of temperature, while the nonradiative decay is strongly affected by the surrounding solvent or host matrix molecules. To reflect the relaxation processes of host matrix more clearly, one can exclude the uncorrelated part, radiative decay, from the fluorescence decay. Extrapolation of the value of fluorescence lifetime  $\tau$  to 0 K gives the value of the radiative lifetime  $\tau_r$ . The nonradiative decay rate  $\tau_{nr}^{-1}$  of MG was obtained by subtracting the radiative decay rate from the fluorescence decay rate  $\tau^{-1}$ ,

$$\tau_{nr}^{-1} = \tau^{-1} - \tau_r^{-1}. \quad (1)$$

As mentioned before, the fluorescence decay curves were well fitted to biexponential functions in a certain temperature range, and the slow decay component exists in the full temperature range investigated in our experiment. Therefore, let us first discuss about the slow decay component. For the three monomers and PB, the Arrhenius plots of the nonradi-

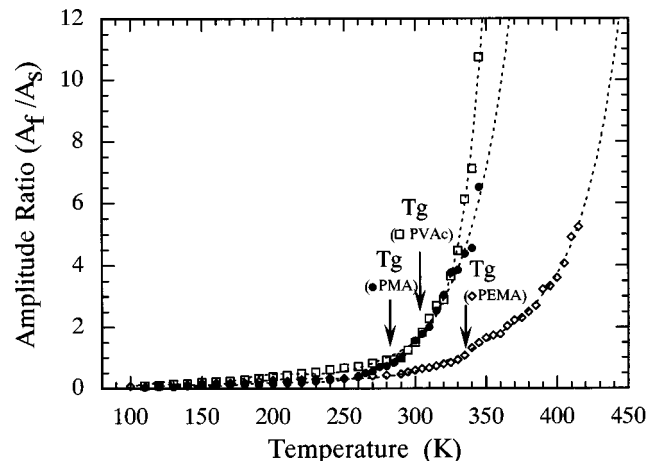


FIG. 8. Amplitude ratios between the fast and slow decay components of MG in PVAc, PMA, and PEMA are shown as functions of temperature.

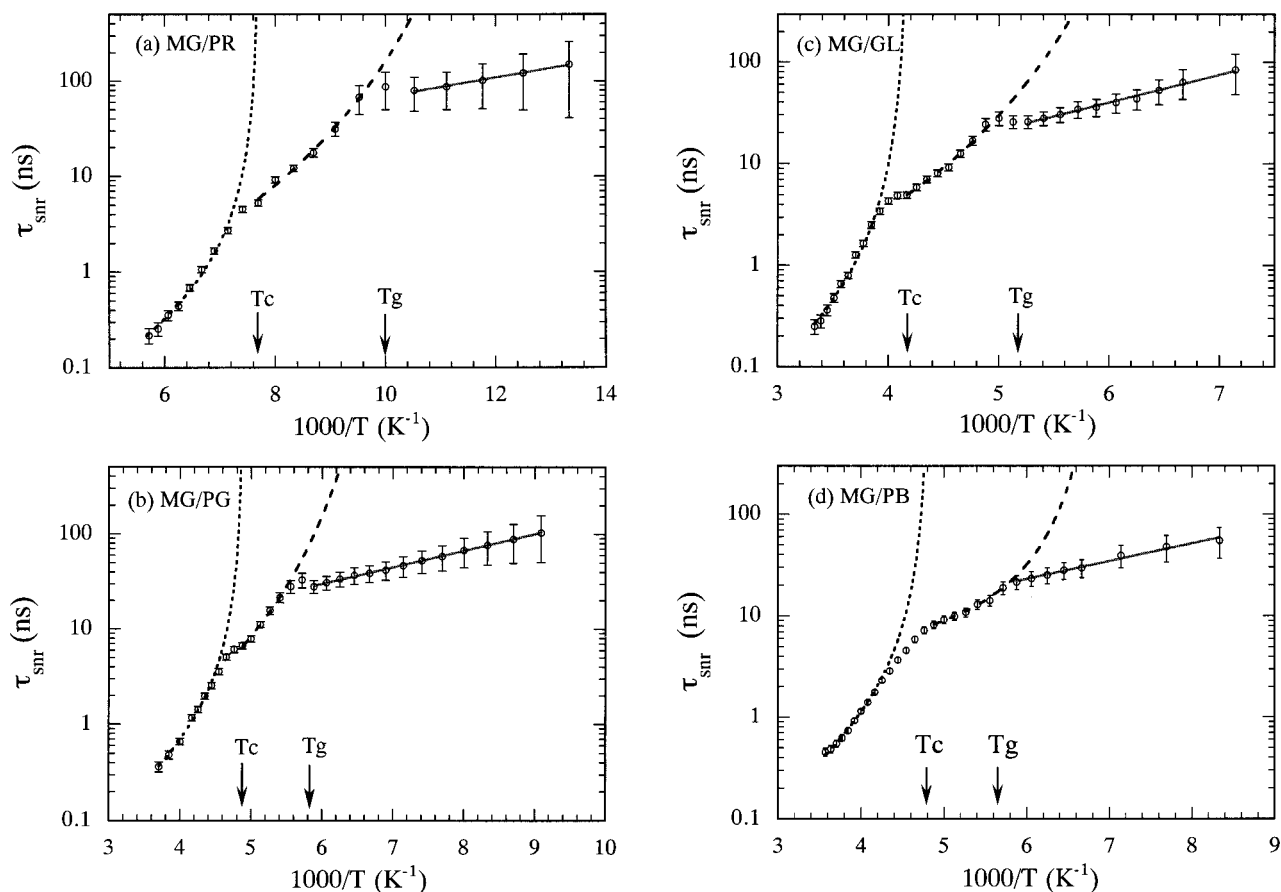


FIG. 9. Arrhenius plots of the nonradiative decay time of the slow component of MG (a) for PR, (b) for PG, (c) for GL, and (d) for PB. The dotted, dashed, and solid lines represent the fitting curves obtained with the power law, VTF equation, and Arrhenius law in the different temperature regions, respectively.

ative decay time of the slow decay component  $\tau_{\text{snr}}$  of doped MG molecules are shown in Fig. 9 with error bars. The similarity between the results of PB and those of the three monomeric samples is obvious. In each curve three temperature regimes are clearly recognized. The lower crossover temperature is located close to the calorimetric glass transition temperature  $T_g$ , and the higher crossover temperature  $T_c$  is about 30–50 K above  $T_g$ . Since  $T_c$  is just in the temperature range where the critical phenomenon is expected to appear by MCT, it is reasonable to attribute it to the critical temperature in the framework of MCT. This experimental finding is notable since the crossover at  $T_c$  is difficult to be observed by the conventional macroscopic measurements. For example, in the temperature dependence of the macroscopic viscosity measured by a normal type viscometer, no kink above  $T_g$  could be observed.<sup>36,37</sup> As predicted by MCT, the crossover at  $T_c$  is caused by a dynamical phase transition, which can be observed only in the relevant dynamical window, i.e., in a mesoscopic time regime and on a microscopic length scale.

The reason why the crossover phenomenon at  $T_c$  has been clearly seen in our experiment can be attributed to the special nature of our probe molecule MG. The nonradiative decay rate of MG is determined by two processes; one is the diffusive rotational motion of the phenyl rings to a sink, and the other is the relaxation from the excited state to the ground state by the internal conversion at the sink. It is well known

that the internal conversion at the sink is very fast for MG and the diffusive rotational motion is the rate-limiting process; then, the nonradiative decay time of MG is proportional to the microscopic viscosity of the surrounding solvent or host matrix molecules.<sup>18,32–34</sup> Furthermore, since the internal potential for the phenyl-ring rotation is known to be barrierless and flat, and the required amount of rotation for the internal conversion to occur is very small, about  $10^\circ$ ,<sup>32</sup> the dynamics of solvents in the supercooled state can be probed in the mesoscopic time window of  $10^{-11}$ – $10^{-8}$  s and on a length scale of several angstroms.<sup>18</sup> This feature is quite different from most of other molecular probes. Depolarization of dye molecules in the glass-forming solvents was measured by Hyde and co-workers with singlet and triplet transient grating techniques,<sup>29,30</sup> and the rotational reorientation dynamics of disperse red 1 in polystyrene was studied by Dhinjwala *et al.* using an experimental protocol involving second harmonic generation.<sup>31</sup> In both experiments the molecular probes rotate as a whole, which is in contrast to the case of MG, where the phenyl rings rotate only a small angle around their bond axes. Moreover, there are many examples of photoisomerization experiments for stilbene, azobenzene, and spirobenzene molecules in polymers.<sup>38–41</sup> The relevant isomerization processes, such as *cis-trans* isomerization, involve large-scale sweeping motions of phenyl rings and other associated components. In all these cases the length scale and time window involved are quite different

from those of the present study, and thus it can be understood that no crossover at  $T_c$  has been found in most of their results, although the dynamics of molecular probes in glass-forming materials has been reported by many researchers.

The fact that in the present study the temperature dependence of  $\tau_{\text{snr}}$  consists of three regimes indicates that the dominant dynamical mode of the surrounding solvent or host matrix molecules which affects the rotational motion of phenyl rings of MG is different in each temperature regime. Therefore, the temperature dependence of the nonradiative decay time was fitted to different equations in different temperature regimes.<sup>42</sup> Above  $T_c$  the nonradiative decay time  $\tau_{\text{snr}}$  was fitted to a power-law equation according to MCT,<sup>2,3</sup>

$$\tau_{\text{snr}} = \tau_H^0 [T_c / (T - T_c)]^\gamma \quad \text{for } T > T_c, \quad (2)$$

where  $\tau_H^0$ ,  $\gamma$ , and  $T_c$  are constants. Free fits of the experimental data by Eq. (2) are not very informative, since the exponent  $\gamma$  depends sensitively on the value used for  $T_c$  and the latter depends on the temperature interval chosen for the fit. From Fig. 9 one can see the curve breaks at a certain temperature higher than  $T_g$ , which serves as a first meaningful guess for the value of  $T_c$ , and by judging the fitting quality with adjusting the value of  $T_c$ , one can fix  $T_c$  to within a few degrees.

The data can be well fitted to Eq. (2), except for the temperature region very close to  $T_c$ , which is reasonable because the thermally activated hopping processes smear out the divergence of the nonradiative decay time. In the extended version of MCT, the divergence of the relaxation time predicted by the idealized version of the theory does not exist.<sup>2,3</sup>

We obtained the values of  $T_c$  to be 130, 205, 240, and 208 K and the values of  $\gamma$  to be 1.75, 1.72, 2.03, and 1.81 for PR, PG, GL, and PB, respectively. Values of  $T_c$  for PG, GL, and PB have also been reported by other authors. A scaling study of the dielectric  $\alpha$  relaxation by Schönhals *et al.*<sup>15</sup> reported  $T_c$  to be 251.3 and 248.8 K for PG and GL, respectively. Light-scattering studies from two groups gave quite different values of the crossover temperature  $T_c$  for GL, i.e.,  $225 \pm 5$  K (Ref. 16) and 310 K.<sup>17</sup> One can see that the reported values are very much scattered, while the values obtained in this study for the monomeric solvents are consistent with each other and consistent with each value of  $T_g$ . On the other hand, as a typical glass-forming polymer with a simple molecular structure, PB has been intensively studied by neutron- and light-scattering measurements, and the results were in good agreement with the predictions of MCT. Richter and co-workers<sup>19</sup> found a singular point at 205 K in the temperature dependence of the nonergodicity parameter corresponding to a critical temperature  $T_c$  in the neutron-spin-echo experiment. Later on Frick and Farago<sup>20</sup> performed a similar experiment, but at a different wave vector, and found the critical temperature  $T_c$  to be about 216 K. In a recent Brillouin light-scattering experiment,<sup>21</sup> the temperature dependence of the velocity of longitudinal phonons showed two singularity points, the first one located at  $T_g$  and the second corresponding to the critical temperature  $T_c$ , about 35 K above  $T_g$ . The value of  $T_c$  found in the present study is consistent with the value obtained by neutron and Brillouin

light-scattering experiments<sup>19–21</sup> within errors and in agreement with the predictions of MCT.

In the temperature range between  $T_g$  and  $T_c$ , the nonradiative decay time was fitted to the Vogel-Tammann-Fulcher (VTF) law

$$\tau_{\text{snr}} = \tau_M^0 \exp[B / (T - T_0)] \quad \text{for } T_c > T > T_g, \quad (3)$$

where  $\tau_M^0$ ,  $B$ , and  $T_0$  are constants. The VTF law was originally established as an empirical equation in 1920s,<sup>43</sup> and more than 30 years later the first derivation of it came out from the free volume theory.<sup>44</sup> Although it could not be deduced in the framework of MCT, the VTF law is still widely used in the supercooled liquid state.<sup>2,15</sup> Here the nonradiative decay time of doped MG molecules in this temperature regime has been fitted to the VTF law, although our data quality is not good enough to determine the specific functional form. We obtained the values of  $T_0$  to be 65, 117, 122, and 137 K, and the values of  $B$  to be 254, 361, 408, and 71 K for PR, PG, GL, and PB, respectively. The values of  $T_0$  agree with those obtained from dielectric relaxation,<sup>35,45</sup> Brillouin light-scattering,<sup>46</sup> specific-heat,<sup>47</sup> ultrasonic,<sup>48</sup> and viscosity measurements<sup>49</sup> within an error of 15 K. This good agreement between different measurements implies that  $T_0$  is an inherent parameter of glass transition of solvent. The characteristic temperature  $T_0$  from the VTF equation was found in most cases to coincide with the Kauzmann temperature where the liquid entropy curve extrapolated below the glass-transition temperature would intersect the crystal entropy curve.<sup>35,50</sup>

On the other hand, the obtained values of parameter  $B$  are much smaller than those from other macroscopic measurements.<sup>35,45–49</sup> This is due to the weak temperature dependence of the nonradiative decay time of doped MG molecules. Since the rotational motions of phenyl rings of MG occur on a microscopic length scale and in a mesoscopic time regime, the motions of surrounding molecules in this relevant dynamical window are monitored. The small value of parameter  $B$  obtained here implies that the rotational motion of phenyl rings of MG is not fully coupled to the motion of solvent on the macroscopic scale. The macroscopic measurements, such as the viscosity measurement, monitor large-scale motion where the breaking of bonds between molecules is involved; therefore, the activation energy corresponding to the motion investigated by the macroscopic measurements is relatively large. On the other hand, the phenyl-ring rotation of our probe molecule is on a microscopic scale; therefore, even some small deformation of the host matrix may result in the phenyl-ring rotation of MG, and this process does not need a large activation energy. From Eq. (3) one can see that parameter  $B$  is a proportional factor of the activation energy. Hence it is reasonable that the values of parameter  $B$  obtained in our measurements are much smaller than those from other macroscopic measurements.

For the temperatures below  $T_g$ , the nonradiative decay time still changes with temperature, and Arrhenius-type temperature dependence has been found, i.e.,

$$\tau_{\text{snr}} = \tau_L^0 \exp[E_a / k_B T] \quad \text{for } T < T_g, \quad (4)$$

where  $\tau_L^0$  is a constant,  $k_B$  Boltzmann constant, and  $E_a$  the activation energy. The fact that the nonradiative decay time of MG in the glassy samples is of Arrhenius-type temperature dependence is consistent with our previous studies.<sup>33,34</sup> Dhinojwala *et al.* also found that below  $T_g$  the rotational reorientation time of disperse red 1 in polystyrene shows an Arrhenius temperature dependence.<sup>31</sup> Below  $T_g$ , the thermally activated hopping stops and molecules are frozen in a certain configuration so that they cannot move around. However, some other freedoms of motions still remain and a small deformation of the network may occur, which affects the diffusive rotational motion of the phenyl rings of MG. Therefore, below  $T_g$ , it is reasonable that the microscopic friction for the rotational motion of phenyl rings has a definite activation energy  $E_a$  for each solvent. The activation energies were obtained to be 1.92, 3.32, and 5.23 kJ/mol for PR, PG, and GL, respectively. The value increases in the order which agrees with the order of the density of hydrogen bonds or the stiffness of network. In case of the PB sample,  $E_a$  was obtained to be 3.35 kJ/mol.

For each of the monomers and PB, a critical phenomenon at  $T_c$  has been observed, which is in agreement with the prediction of MCT. It is interesting to check whether MCT universally applies to various kinds of glass-forming materials independent of their chemical structures. To address this question, we have investigated the dynamics of the glass transition of PVAc, PMA, and PEMA polymeric samples by means of time-resolved fluorescence measurement. PVAc, PMA, and PEMA are typical glass-forming polymers, which contain side chains unlike PB. The nonradiative decay time of the slow decay component of doped MG in these three samples was obtained by subtracting the radiative decay part from the fluorescence decay. Figure 10 shows the Arrhenius plots of the nonradiative decay time as functions of temperature. For each sample the nonradiative decay time at  $T_g$  is about 10 times shorter than those for the monomers and PB, a polymer without side chains. This may be due to the fact that even below  $T_g$  the side-chain motions have not been frozen in yet, so that the microscopic viscosity experienced by MG molecules is not so large as those for monomers and PB at their  $T_g$ 's. Many other studies also support this idea that the side chains are still moving even when the main chain is frozen in below  $T_g$ .<sup>51-53</sup>

For each curve in Fig 10, a kink can be seen at  $T_g$ , although it is not so pronounced as those for the monomeric samples and PB. However, no singular point could be clearly distinguished above  $T_g$ ; i.e., we could not find the crossover at  $T_c$ , which, even if it exists, may be masked by the side-chain motions. One must remember that MCT has been originally developed for atomic fluids; therefore, its applicability to the complex polymer systems is still a question open to debate. The temperature behavior of the relaxation processes of poly(*n*-butyl acrylate) investigated by dielectric spectroscopy<sup>22</sup> and Brillouin light scattering<sup>23</sup> was found not to be in accordance with the predictions of MCT. The dynamics of the  $\alpha$  relaxation in poly(vinyl methyl ether) has been studied by means of dielectric and mechanical spectroscopies and nuclear magnetic resonance, as well as quasi-elastic neutron-scattering measurements, but no direct hint for a critical temperature from the temperature behavior of the characteristic time scale of the  $\alpha$  process was found.<sup>24</sup> On

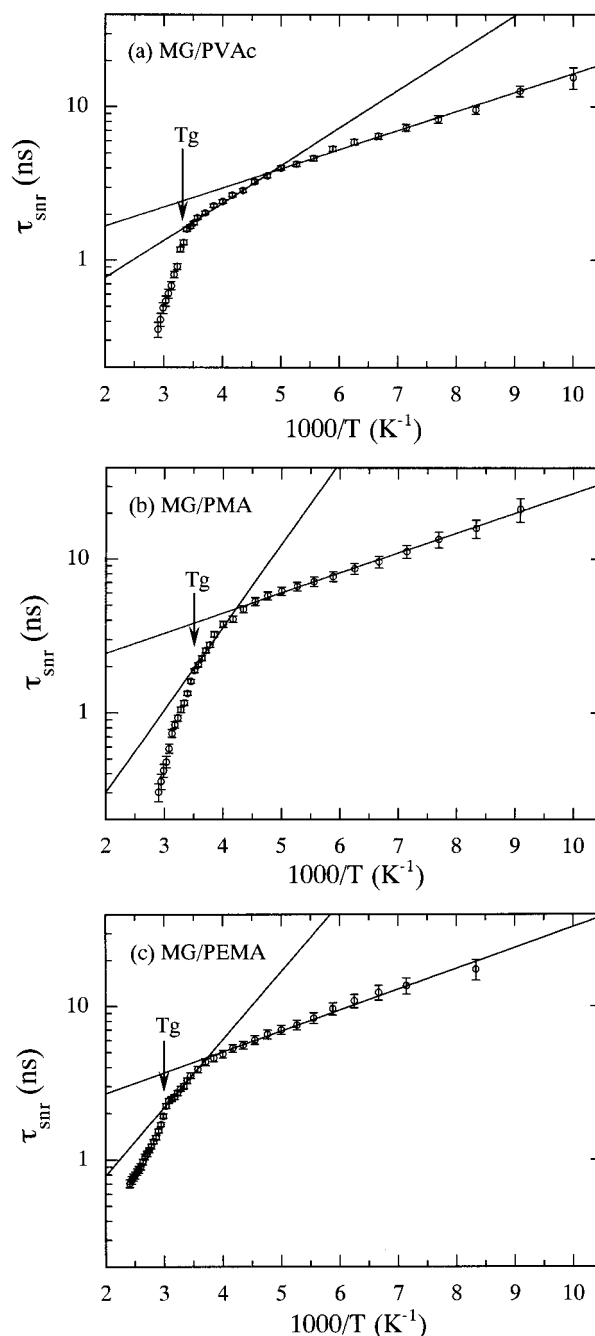


FIG. 10. Arrhenius plots of the nonradiative decay time of the slow component of MG (a) for PVAc, (b) for PMA, and (c) for PEMA. Below  $T_g$  the data were found to have two regions of Arrhenius temperature dependence.

the other hand, the dynamics in the glass-transition region of PVAc and a blend of PVAc and poly(4-hydroxystyrene) have been studied using dynamic-mechanical and light-scattering measurements, and it was claimed that the result was in agreement with the predictions of MCT, although  $T_c < T_g$  was obtained in their experiment.<sup>25</sup> In the present study, the fact that no crossover temperature above  $T_g$  has been found may result from the overlapping of the  $\alpha$  process and the side-chain motions; i.e., the side-chain motions may mask the subtle crossover at  $T_c$ . However, as mentioned by Götze and Sjögren, in the case of polymers, if no anomaly is found above  $T_g$ , one cannot conclude much, since the chosen dy-

namical window might just be wrong.<sup>2</sup> Nevertheless, since the same molecular probe has been used in the present study for different types of glass formers, at least one conclusion may be drawn from our experimental findings; i.e., in the same dynamical window, different relaxation behavior has been observed for the complex polymers with side chains, such as PVAc, PMA, and PEMA, although the dynamics of the glass transition of PB, a polymer without side chains, was found to be similar to that of monomeric glass formers.

On the other hand, as is shown in Fig. 10 the Arrhenius plot of  $\tau_{\text{snr}}$  is not a single straight line below  $T_g$ , but has two Arrhenius-type temperature-dependent regions separated by a kink at a temperature several tens of degrees below  $T_g$ . One should notice that all the PVAc, PMA, and PEMA samples contain ester side chains. The relaxation of polymers due to the local motions of ester side chains has been studied by dynamic mechanical measurements,<sup>51,54,55</sup> dielectric relaxation measurements,<sup>51</sup> and nuclear magnetic resonance measurements.<sup>53</sup> The results of those studies showed that the reorientation of ester side chain occurs even below  $T_g$ . Therefore, the kink observed in the present study at several tens of degrees below  $T_g$  may be attributed to the freezing of the rotation of ester groups. In the temperature region below the kink, the nonradiative decay time of doped MG molecules still changes with temperature, which implies that some kind of relaxation process still exists so that the host molecules have not been completely frozen in yet. Hindered rotation of ester methyl group in poly(methyl acrylate) and poly(methyl methacrylate) was found even at 77 K by means of nuclear magnetic resonance measurements.<sup>53</sup>

In the above we have shown that the dynamics of complex polymers is different from that of the monomers and PB, since the side-chain motion plays an important role in the microscopic dynamics. On the other hand, we found that the dynamics of PB, a polymer without side chains, is similar to that of the monomeric glass-forming solvents. PB is a polymer, and therefore its molecular structure is different from that of the monomers. However, since PB has a very simple structure composed of a backbone without side chains, the degree of motion of the molecule is limited to that of the backbone. In cases of small monomers, translational motion is essential in the supercooled liquid state. Therefore, from the fact that relatively simple motion determines the dynamics of both the monomers and PB, it seems easy to understand our experimental finding of the similarity of the dynamics between the monomers and PB.

Besides the slow decay component discussed in the above, a fast decay component has also been observed in a certain temperature range for each sample used in the present study. To discuss the nature of the fast decay in different samples, the Arrhenius plots of the nonradiative decay time of the fast decay component of MG in the three monomers and PB are shown in Fig. 11 as functions of temperature. The fast decay processes only appear in the liquid state and become faster with increasing temperature. The similarities between these samples imply that there is a common origin for the fast decay processes. It is well known that inhomogeneities are very large in the supercooled state.<sup>56-62</sup> Light-scattering experiments indicate that the physical origin of the nonexponential character of structural relaxation is caused by the nanoscale inhomogeneities,<sup>56,57</sup> and two different relax-

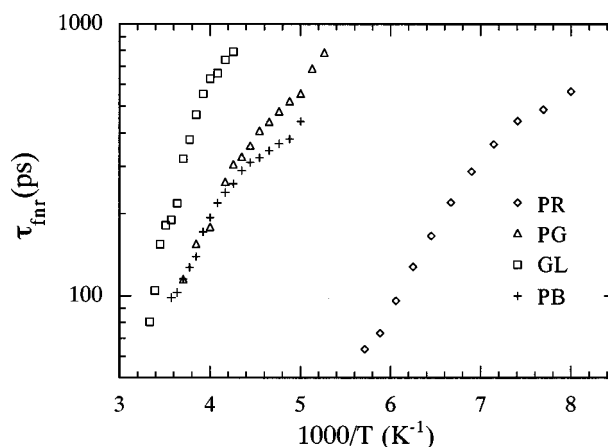


FIG. 11. Arrhenius plots of the nonradiative decay time of the fast component of MG in PR, PG, GL, and PB as functions of temperature.

ation mechanisms of liquidlike and solidlike sites coexisting in the glass-transition regime were found by electron-spin-resonance measurements.<sup>58</sup> In the present study the fast decay component, we think, may arise from the liquidlike sites, i.e., the noncooperative or weakly cooperative region, while the slow decay component may come from the solidlike sites, i.e., the strongly cooperative region. It should be noted here that the fast processes in different measurements may have different origins, and the assignment of fast processes is still a question of much controversy.<sup>63,64</sup> Within the framework of MCT, the fast process, namely, the  $\beta$  process, which is caused by the inside-cage relaxation, exists both above and below  $T_c$ .<sup>2,3</sup> Moreover, the  $\beta$  process was found to be on a picosecond or subpicosecond time scale by means of neutron- and light-scattering measurements.<sup>11,12,65</sup> The fast process observed in the present study is in a much longer time regime and only appears in the liquid state; therefore, it may not correspond to the  $\beta$  process of MCT, while it can be more reasonably attributed to the inhomogeneities of supercooled liquids.

The temperature dependence of the nonradiative decay time of the fast decay component of MG in PVAc, PMA, and PEMA is shown in an Arrhenius plot (see Fig. 12), which is

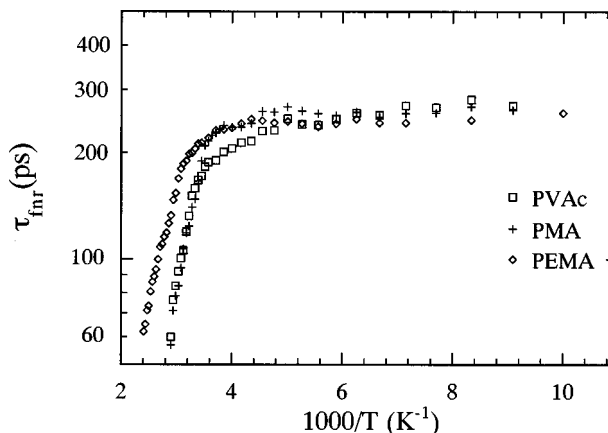


FIG. 12. Arrhenius plots of the nonradiative decay time of the fast component of MG in PVAc, PMA, and PEMA as functions of temperature.



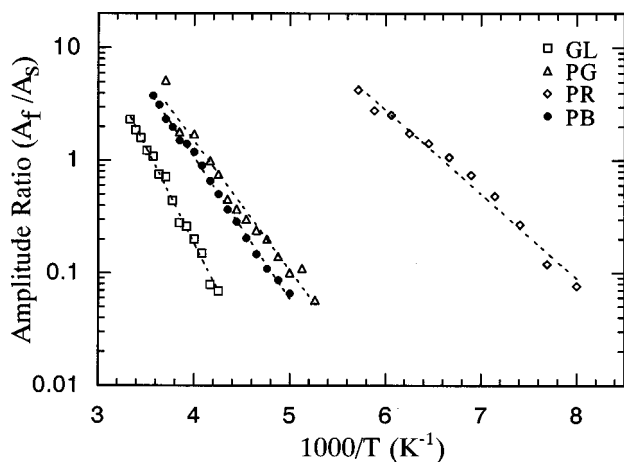


FIG. 13. Arrhenius plots of the amplitude ratios between the fast and slow components as functions of temperature for MG in PR, PG, GL, and PB.

different from those of PB and the monomeric samples. For each of the complex polymer samples, the fast decay component exists even far below  $T_g$ . This experimental finding can be understood by taking into account the fact that for the complex polymers, although the translational motion stops at  $T_g$ , the side-chain motion still remains, so that even below  $T_g$  the complex polymer is not so stiff, especially seen by the very small molecular probe, and some flexible sites can remain at very low temperatures. Below  $T_g$  the fast decay component of MG in the complex polymer matrix has a very weak temperature dependence, which implies that the fast decay process is related to a very local motion. The matrix of a polymer with side chains, such as PVAc, PMA, and PEMA, has a very loose structure even below  $T_g$  if seen by a microscopic probe, and the fast decay component may arise from the sites where MG molecules sit in the rather flexible region, i.e., liquidlike sites of the host matrix. At these sites, the phenyl rings can rotate rather freely in the matrix with relatively small activation energy. If the activation energy is smaller than  $k_B T$ , it is consistent with the very weak temperature dependence of the decay time.

From the above discussion of the slow and fast decay components of doped MG molecules, it is clearly revealed by our experiment that the dynamics taking place in the complex polymers with side chains is different from that of the monomeric samples or a polymer without side chains. For a further discussion, let us see the amplitude ratios between the fast and slow decay components of MG in these samples. The Arrhenius plots of the amplitude ratios as functions of temperature are shown in Fig. 13 for PB and the monomer samples and in Fig. 14 for PVAc, PMA, and PEMA.

In cases of PB and the monomers, the amplitude of the slow decay component is much smaller than that of the fast decay component at high temperatures, but it increases with lowering temperature. When the temperature approaches  $T_g$ , the slow decay component becomes the dominant one, and the decay curve is practically well fitted to a single-exponential function. Therefore, the biexponential decay is essentially only in the supercooled state. This result further supports the idea that the two decay components may come from the liquidlike and solidlike sites. It indicates that the volume of the solidlike site grows with decreasing tempera-

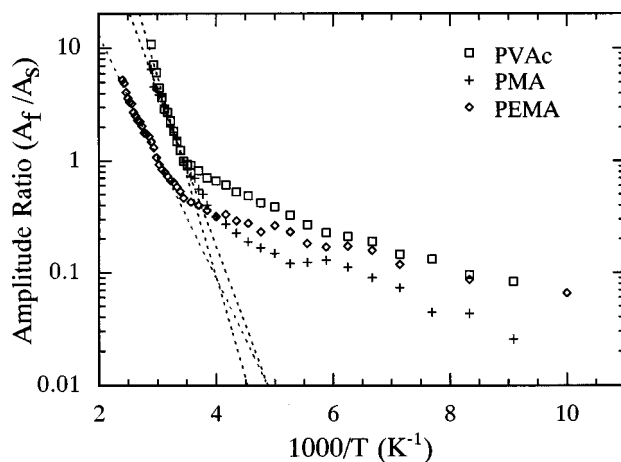


FIG. 14. Arrhenius plots of the amplitude ratios between the fast and slow components as functions of temperature for MG in PVAc, PMA, and PEMA.

ture and finally covers all the sample in the vicinity of  $T_g$ , while the liquidlike site changes with temperature in the opposite way; i.e., it starts to appear near  $T_g$  and increases with temperature until it prevails in the high temperatures. The amplitude ratios for these samples are of Arrhenius-type temperature dependence, and by fitting the data we obtained the free energy differences between the fast and slow sites, which are 24.1, 14.8, 21.2, and 32.4 kJ/mol for PB, PR, PG, and GL, respectively. For each of the complex polymer samples shown in Fig. 14, the fast decay component of doped MG remains at very low temperatures. Below  $T_g$  the ratio slowly reduces with decreasing temperature, while it changes dramatically at the high-temperature regime. The data above  $T_g$  roughly fall on a straight line, and we obtained the free energy difference between the fast and slow sites to be 34.2, 26.8, and 20.7 kJ/mol for PVAc, PMA, and PEMA, respectively.

Sharp contrast between Figs. 13 and 14 can be clearly seen. As was previously discussed, a remarkable difference has also been found for the temperature dependence of the nonradiative decay time of the slow or the fast decay component between the complex polymers with side chains and the monomers or the polymer without side chains. The difference of the temperature dependence of the amplitude ratios between the two groups of samples shown in Figs. 13 and 14 is in accordance with the results discussed above and can be attributed to the same origin, i.e., the different chemical structures between the glass-forming materials.

## V. CONCLUSIONS

In conclusion, the dynamics of the glass transition of several monomeric and polymeric glass-forming materials has been investigated by the time-resolved fluorescence measurements of doped MG molecules in a wide temperature region. The nonradiative decay time of MG sensitively reflects the relaxation processes of glass-forming materials. For each of the monomers and a polymer without side chains, besides a kink around  $T_g$ , another crossover at  $T_c$ , about 30–50 K above  $T_g$ , has been clearly observed. This experimental finding gives a strong support to MCT which predicts such a dynamical anomaly above the calorimetric glass-

transition temperature  $T_g$ . Moreover, fast and slow relaxation processes were found to coexist in the supercooled state, which has been attributed to the inhomogeneities of the glass formers in the temperature region. The similarity of the results between the monomeric samples and PB, a polymer without side chains, indicates that the dynamics of the glass transition in these samples has a common origin.

On the other hand, for the complex polymers containing side chains the crossover at  $T_g$  is less pronounced than those for PB and the monomeric samples. Furthermore, unlike PB and the monomeric samples, no singular point above  $T_g$  could be clearly distinguished from the temperature dependence of the nonradiative decay time of the slow decay component of doped MG; i.e., we could not find the crossover at  $T_c$  for the complex polymers. The appearance of the singular point at  $T_c$  may be masked by the side-chain motions of the complex polymers. However, a kink at a temperature several tens of degrees below  $T_g$  was found, which was attributed to the motions of ester side chains. In addition, a fast decay process was found to remain even far below  $T_g$  for the complex polymers, whereas the fast decay process only appears from a temperature somewhat above  $T_g$  for the monomers and PB, a polymer without side chains. All of these experimental findings indicate that the microscopic dynamics taking place in the monomers or the polymer without side

chains is different from that in the complex polymers with side chains.

In the monomers or the polymer without side chains, there are essentially only the translational or the main-chain motions of the solvent molecules; therefore, it is not strange that the microscopic dynamics of glass transition of PB is similar to that of monomeric samples, although PB is a typical polymer. On the other hand, in the complex polymers with side chains there are other side-chain motions besides the main-chain motions; therefore, it can be understood that the microscopic dynamics of the complex polymers with side chains is not only different from that of the monomeric samples, but also different from that of PB, a polymer without side chains.

The present study illustrates that, due to its special nature, MG serves as a good local probe to investigate the dynamics of the glass transition at a molecular level and on a mesoscopic time scale.

#### ACKNOWLEDGMENT

We are indebted to Professor Seiji Kojima of University of Tsukuba for extensive discussion and for providing us with the purified monomer solvents.

- 
- \*Present address: Joint Research Center for Atom Technology, Angstrom Technology Partnership, National Institute for Advanced Interdisciplinary Research, 1-1-4 Higashi, Tsukuba, Ibaraki 305, Japan.
- <sup>1</sup>U. Bengtzelius, W. Götze, and A. Sjölander, *J. Phys. C* **17**, 5915 (1984); E. Leutheusser, *Phys. Rev. A* **29**, 2765 (1984).
  - <sup>2</sup>W. Götze and L. Sjögren, *Rep. Prog. Phys.* **55**, 241 (1992).
  - <sup>3</sup>W. Götze, in *Liquids, Freezing and the Glass Transition*, edited by J. P. Hansen, D. Levesque, and J. Zinn-Justin (North-Holland, Amsterdam, 1991), p. 287.
  - <sup>4</sup>F. Mezei, W. Knaak, and B. Farago, *Phys. Rev. Lett.* **58**, 571 (1987).
  - <sup>5</sup>W. Knaak, F. Mezei, and B. Farago, *Europhys. Lett.* **7**, 529 (1988).
  - <sup>6</sup>L. Borjesson, M. Elmroth, and L. M. Torell, *Chem. Phys.* **149**, 209 (1990).
  - <sup>7</sup>L. Borjesson and W. S. Howells, *J. Non-Cryst. Solids* **131-133**, 53 (1991).
  - <sup>8</sup>M. Kiebel, E. Bartsch, O. Debus, F. Fujara, W. Petry, and H. Sillescu, *Phys. Rev. B* **45**, 10 301 (1992).
  - <sup>9</sup>J. Wuttke, M. Kiebel, E. Bartsch, F. Fujara, W. Petry, and H. Sillescu, *Z. Phys. B* **91**, 375 (1993).
  - <sup>10</sup>H. Z. Cummins, W. M. Du, M. Fuchs, W. Götze, S. Hildebrand, A. Latz, G. Li, and N. J. Tao, *Phys. Rev. E* **47**, 4223 (1993).
  - <sup>11</sup>G. Li, W. M. Du, X. K. Chen, H. Z. Cummins, and N. J. Tao, *Phys. Rev. A* **45**, 3867 (1992).
  - <sup>12</sup>W. M. Du, G. Li, H. Z. Cummins, M. Fuchs, J. Toulouse, and L. A. Knauss, *Phys. Rev. E* **49**, 2192 (1994).
  - <sup>13</sup>M. Elmroth, L. Borjesson, and L. M. Torell, *Phys. Rev. Lett.* **68**, 79 (1992).
  - <sup>14</sup>W. Steffen, A. Patkowski, H. Gläser, G. Meier, and E. W. Fischer, *Phys. Rev. E* **49**, 2992 (1994).
  - <sup>15</sup>A. Schönhal, F. Kremer, A. Hofmann, E. W. Fischer, and E. Schlosser, *Phys. Rev. Lett.* **70**, 3459 (1993).
  - <sup>16</sup>J. Wuttke, J. Hernandez, G. Li, G. Coddens, H. Z. Cummins, F. Fujara, W. Petry, and H. Sillescu, *Phys. Rev. Lett.* **72**, 3052 (1994).
  - <sup>17</sup>E. Rössler, A. P. Sokolov, A. Kisliuk, and D. Quitmann, *Phys. Rev. B* **49**, 14 967 (1994).
  - <sup>18</sup>J. Y. Ye, T. Hattori, H. Inouye, H. Ueta, H. Nakatsuka, Y. Maruyama, and M. Ishikawa, *Phys. Rev. B* **53**, 8349 (1996).
  - <sup>19</sup>D. Richter, B. Frick, and B. Farago, *Phys. Rev. Lett.* **61**, 2465 (1988).
  - <sup>20</sup>B. Frick and B. Farago, *Phys. Rev. Lett.* **64**, 2921 (1990).
  - <sup>21</sup>D. Fioretto, L. Palmieri, G. Socino, and L. Verdini, *Phys. Rev. B* **50**, 605 (1994).
  - <sup>22</sup>D. Fioretto, A. Livi, P. A. Rolla, G. Socino, and L. Verdini, *J. Phys. Condens. Matter* **6**, 5295 (1994).
  - <sup>23</sup>D. Fioretto, G. Carlotti, L. Palmieri, G. Socino, L. Verdini, and A. Lini, *Phys. Rev. B* **47**, 15 286 (1993).
  - <sup>24</sup>J. Colmenero, A. Alegria, J. M. Alberdi, and F. Alvarez, *Phys. Rev. B* **44**, 7321 (1991).
  - <sup>25</sup>G. Luengo, F. Ortega, R. G. Rubio, A. Rey, M. G. Prolongo, and R. M. Masegosa, *J. Chem. Phys.* **100**, 3258 (1993).
  - <sup>26</sup>G. J. Blanchard, *J. Chem. Phys.* **87**, 6802 (1987).
  - <sup>27</sup>L. J. Miller and A. M. North, *J. Chem. Soc. Faraday Trans. 2* **71**, 1233 (1975).
  - <sup>28</sup>B. Nayak and S. N. Gupta, *J. Polym. Sci. Polym. Chem. Ed.* **33**, 891 (1995).
  - <sup>29</sup>P. D. Hyde, T. E. Evert, and M. D. Ediger, *J. Chem. Phys.* **93**, 2274 (1990).
  - <sup>30</sup>P. D. Hyde, T. E. Evert, M. T. Cicerone, and M. D. Ediger, *J. Non-Cryst. Solids* **131-133**, 42 (1991).
  - <sup>31</sup>A. Dhinojwala, G. K. Wong, and J. M. Torkeson, *J. Chem. Phys.* **100**, 6046 (1994).
  - <sup>32</sup>D. Ben-Amotz and C. B. Harris, *J. Chem. Phys.* **86**, 4856 (1987); **86**, 5433 (1987); D. Ben-Amotz, R. Jeanloz, and C. B. Harris, *ibid.* **86**, 6119 (1987).

- <sup>33</sup>K. M. Abedin, J. Y. Ye, H. Inouye, T. Hattori, and H. Nakatsuka, *J. Lumin.* **64**, 135 (1995).
- <sup>34</sup>K. M. Abedin, J. Y. Ye, H. Inouye, T. Hattori, H. Sumi, and H. Nakatsuka, *J. Chem. Phys.* **103**, 6414 (1995).
- <sup>35</sup>C. A. Angell and D. L. Smith, *J. Phys. Chem.* **86**, 3845 (1982).
- <sup>36</sup>V. G. Tammann and W. Hesse, *Z. Anorg. Allg. Chem.* **156**, 245 (1926); J. S. Hutzler, R. J. Colton, and A. C. Ling, *J. Chem. Eng. Data* **17**, 324 (1972); R. Piccirelli and T. A. Litovitz, *J. Acoust. Soc. Am.* **29**, 1009 (1957).
- <sup>37</sup>G. C. Berry and T. G. Fox, *Adv. Polym. Sci.* **5**, 261 (1968).
- <sup>38</sup>C. S. P. Sung, L. Lamare, and M. K. Tse, *Macromolecules* **12**, 666 (1979).
- <sup>39</sup>K. Horie, M. Tsukamoto, and I. Mita, *Eur. Polym. J.* **21**, 805 (1985).
- <sup>40</sup>K. Horie, K. Hirao, N. Kenmochi, and I. Mita, *Macromol. Chem. Rapid Commun.* **9**, 267 (1988).
- <sup>41</sup>T. Naito, K. Horie, and I. Mita, *Macromolecules* **24**, 2907 (1991).
- <sup>42</sup>The summation of three functions was used to fit the data of monomeric samples in our previous paper; see Ref. 18. To make the physical meaning of the fitting more clear, in the present paper we use three separated functions to fit the data in different temperature regions.
- <sup>43</sup>H. Vogel, *Phys. Z.* **22**, 645 (1921); G. Tammann and G. Hesse, *Z. Anorg. Allg. Chem.* **156**, 245 (1926); G. S. Fulcher, *J. Am. Chem. Soc.* **8**, 339 (1925).
- <sup>44</sup>M. H. Cohen and D. Turnbull, *J. Chem. Phys.* **31**, 1164 (1959).
- <sup>45</sup>D. W. Davidson and R. H. Cole, *J. Chem. Phys.* **19**, 1484 (1951).
- <sup>46</sup>Z. Hu, J. J. Vanderwal, and D. Walton, *Phys. Rev. A* **37**, 4507 (1988).
- <sup>47</sup>N. O. Birge, *Phys. Rev. B* **34**, 1631 (1986).
- <sup>48</sup>Y. H. Jeong and S. R. Nagel, *Phys. Rev. A* **34**, 602 (1986).
- <sup>49</sup>G. C. Berry and T. G. Fox, *Adv. Polym. Sci.* **5**, 261 (1968).
- <sup>50</sup>T. Odagaki, *Phys. Rev. Lett.* **75**, 3701 (1995).
- <sup>51</sup>G. D. Smith, F. Liu, W. Devereaux, and R. H. Boyd, *Macromolecules* **25**, 703 (1992).
- <sup>52</sup>G. D. Smith and R. H. Boyd, *Macromolecules* **24**, 2731 (1991).
- <sup>53</sup>K. M. Sinnott, *J. Polym. Sci.* **42**, 3 (1960).
- <sup>54</sup>H. W. Starkweather, *Macromolecules* **21**, 1798 (1988); *Polymer* **32**, 2443 (1991).
- <sup>55</sup>E. Donth, in *Relaxation and Thermodynamics in Polymers: Glass Transition*, edited by H. Höpcke (Akademie Verlag, Berlin, 1992), p. 200.
- <sup>56</sup>C. T. Moynihan and J. Schroeder, *J. Non-Cryst. Solids* **160**, 52 (1993).
- <sup>57</sup>J. Schroeder, M. A. Whitmore, M. R. Silvestri, S. K. Saha, and C. T. Moynihan, *J. Non-Cryst. Solids* **161**, 157 (1991).
- <sup>58</sup>J. I. Spielberg and E. Gelerinter, *Phys. Rev. B* **30**, 2319 (1984).
- <sup>59</sup>M. Grimsditch and N. Rivier, *Appl. Phys. Lett.* **58**, 2345 (1991).
- <sup>60</sup>U. Mohanty, *J. Chem. Phys.* **100**, 5905 (1994).
- <sup>61</sup>G. Adam and J. H. Gibbs, *J. Chem. Phys.* **43**, 139 (1965).
- <sup>62</sup>M. H. Cohen and G. S. Grest, *Phys. Rev. B* **20**, 1077 (1979).
- <sup>63</sup>T. Kanaya, T. Kawaguchi, and K. Kaji, *J. Non-Cryst. Solids* **172-174**, 327 (1994).
- <sup>64</sup>E. Rössler, *Phys. Rev. Lett.* **69**, 1620 (1992).
- <sup>65</sup>D. Richter, R. Zorn, B. Farago, B. Frick, and L. J. Fetters, *Phys. Rev. Lett.* **68**, 71 (1992).